

How our Nuclear Star Cluster formed and grew due to first generation globular clusters disruption

by

Maryna Ishchenko

Main Astronomical Observatory,

National Academy of Sciences of Ukraine

Nicolaus Copernicus Astronomical Centre Polish Academy of Sciences

Fesenkov Astrophysical Institute, Kazakhstan

Cosmology 2025,

Elba Island

Nuclear Star Cluster (NSC) are common stellar systems in the centres of galaxies. Yet, the physical mechanisms involved in their formation are still debated.

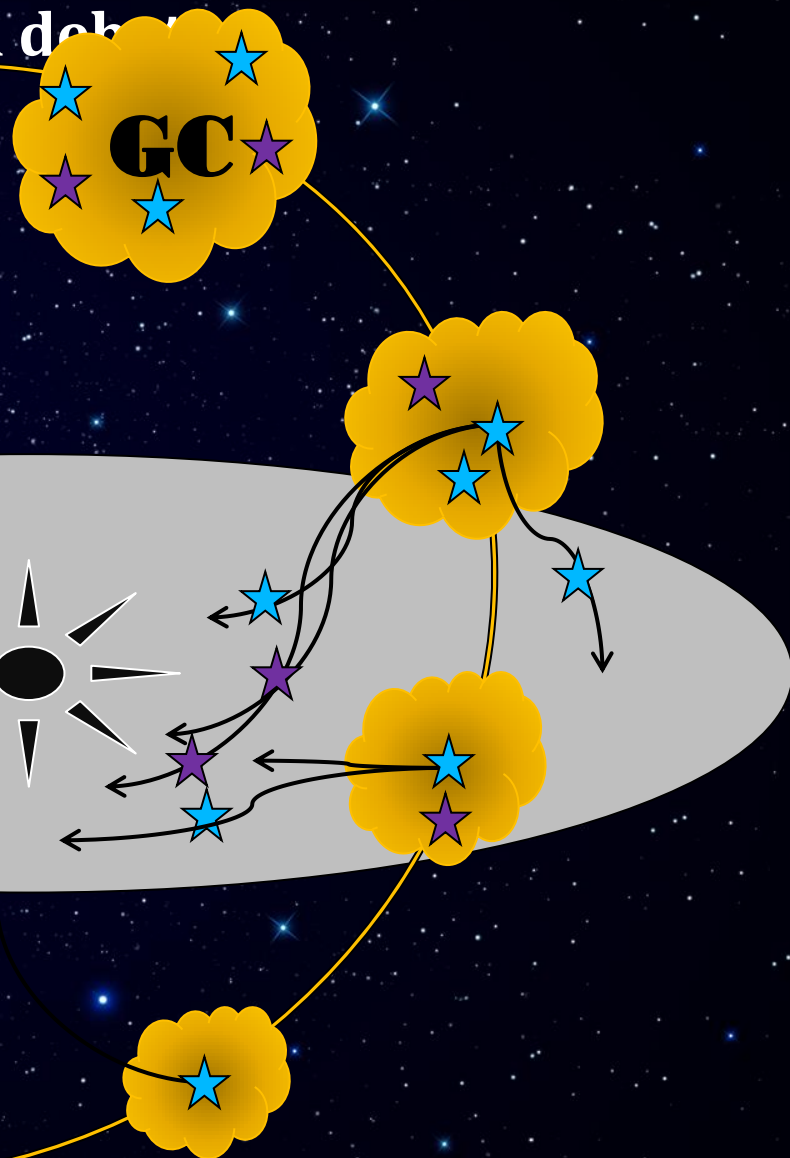
Two formation mechanisms were proposed: the accretion of stellar clusters onto galactic center (cluster-inspiral) and in-situ star formation driven by dissipation of gaseous clouds.

$$M_{\text{NSC}} = 4 \times 10^7 M_{\odot}$$
$$R_{\text{NSC}} = 4 \text{ pc}$$
$$M_{\text{SMBH}} = 4.1 \times 10^6 M_{\odot}$$



GC's stars
high mass remnants (BH + NS)

GC's orbit

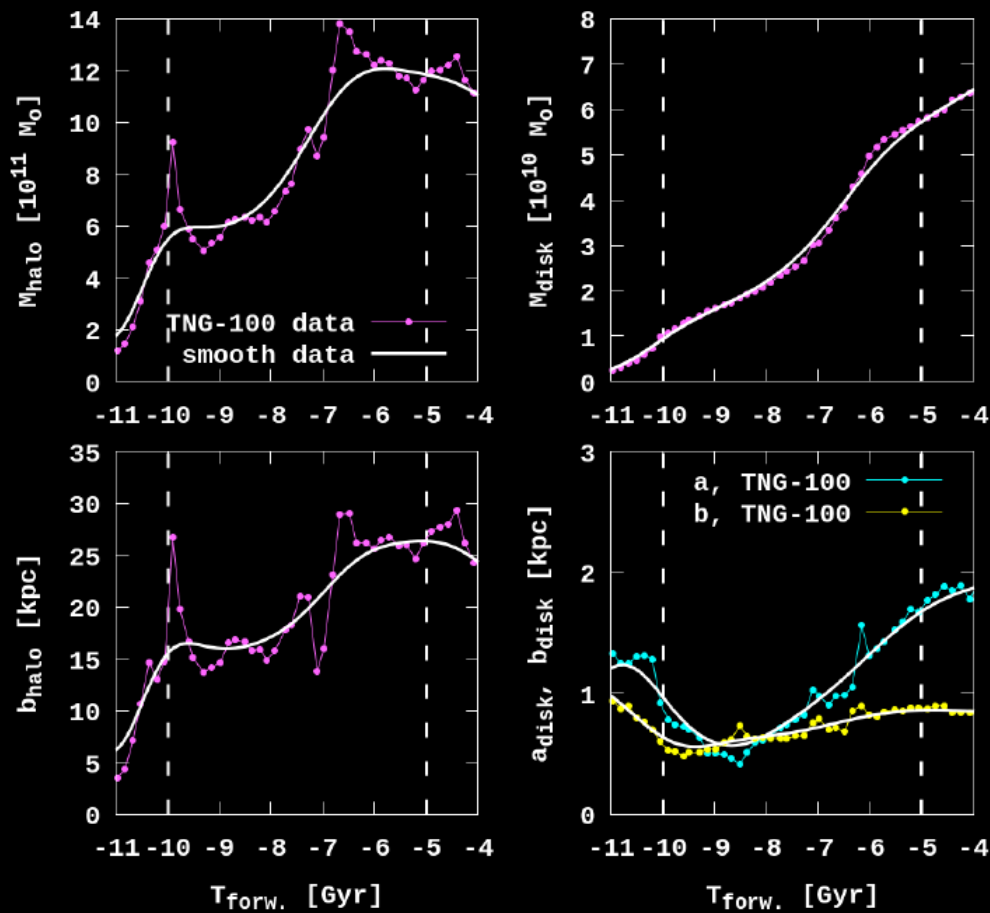
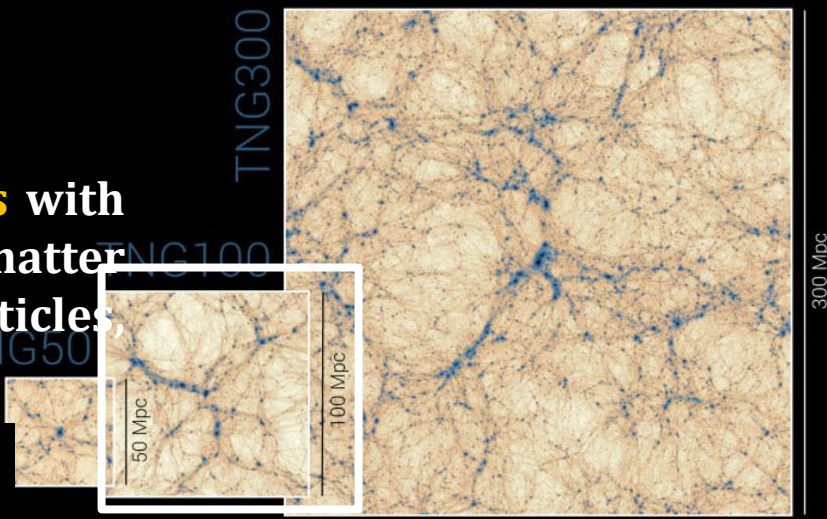


From the general point of view, GCs that can potentially lead to the process of NSC formation in our Galaxy have clearly already been destroyed by these long and dynamically violent processes (Capuzzo-Dolcetta 1993; Antonini 2013; Minniti et al. 2021).

The main idea of this work is investigate the **accretion of GC stars on early cosmological timescales** through detailed N -body simulations of theoretical GC models, in order to assess the role of this mechanism in Milky Way nuclear star cluster formation.

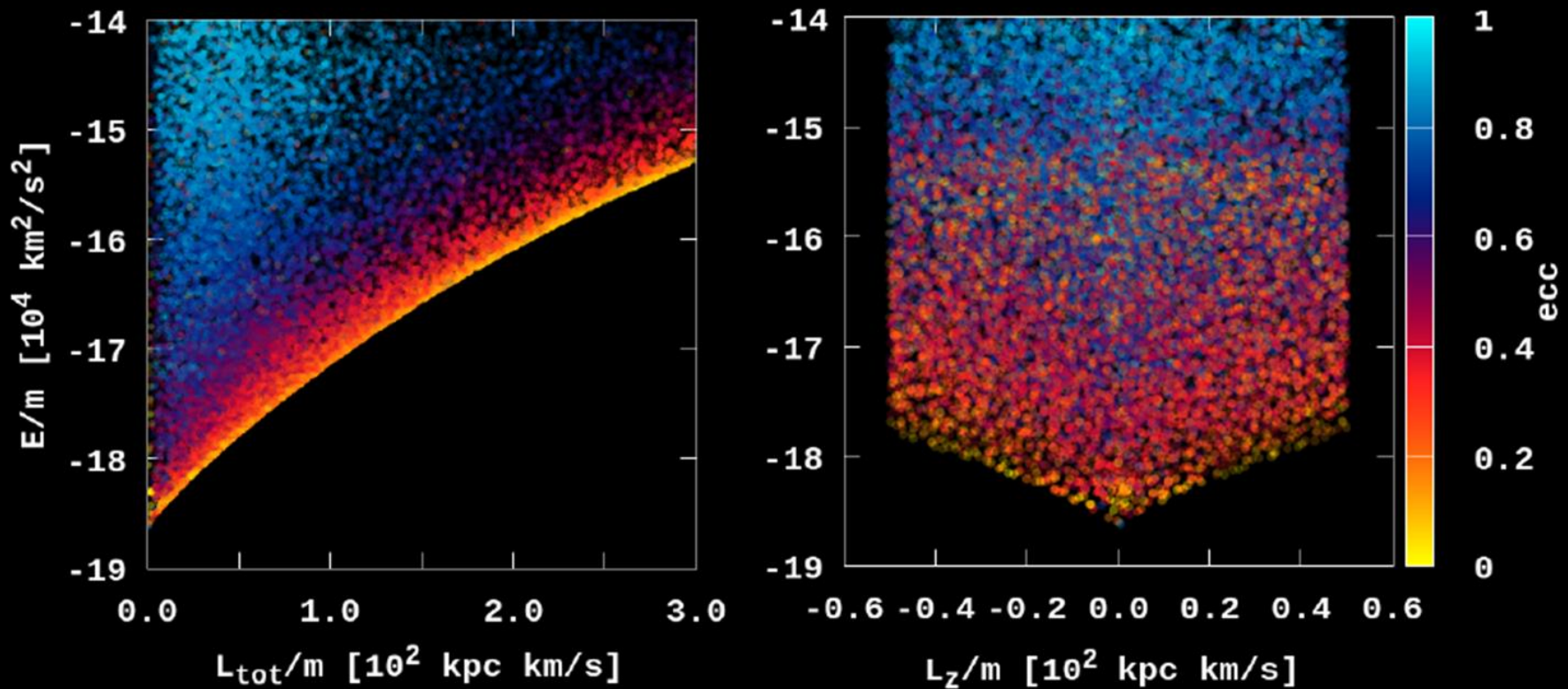
To be more physically realistic in our investigation, we performed our integration of GCs' evolution **in time-varying Milky Way-like potentials**.

The IllustrisTNG-100 is characterized by a simulation box $\sim 100 \text{ Mpc}^3$. In a box of such size **we resolve a 54 MW-mass disk galaxies** with the mass resolution $7,5 \times 10^6 M_{\odot}$ for dark matter and $1,4 \times 10^6 M_{\odot}$ for the baryonic particles, respectively.



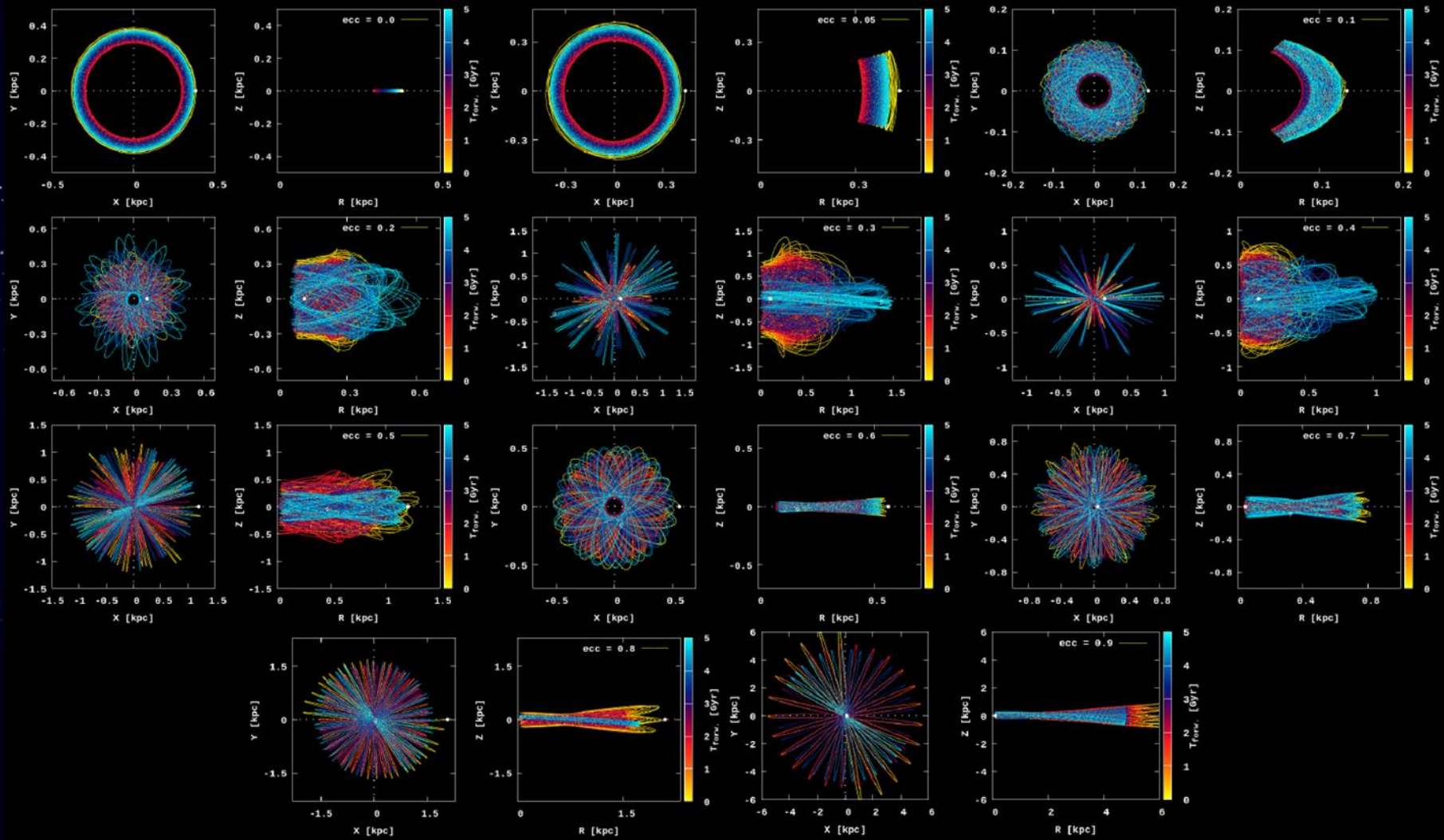
Magenta dot-dashed lines correspond to the original data from IllustrisTNG-100.

Evolution of halo and disk masses, and their characteristic scales for **#411321 in time.**

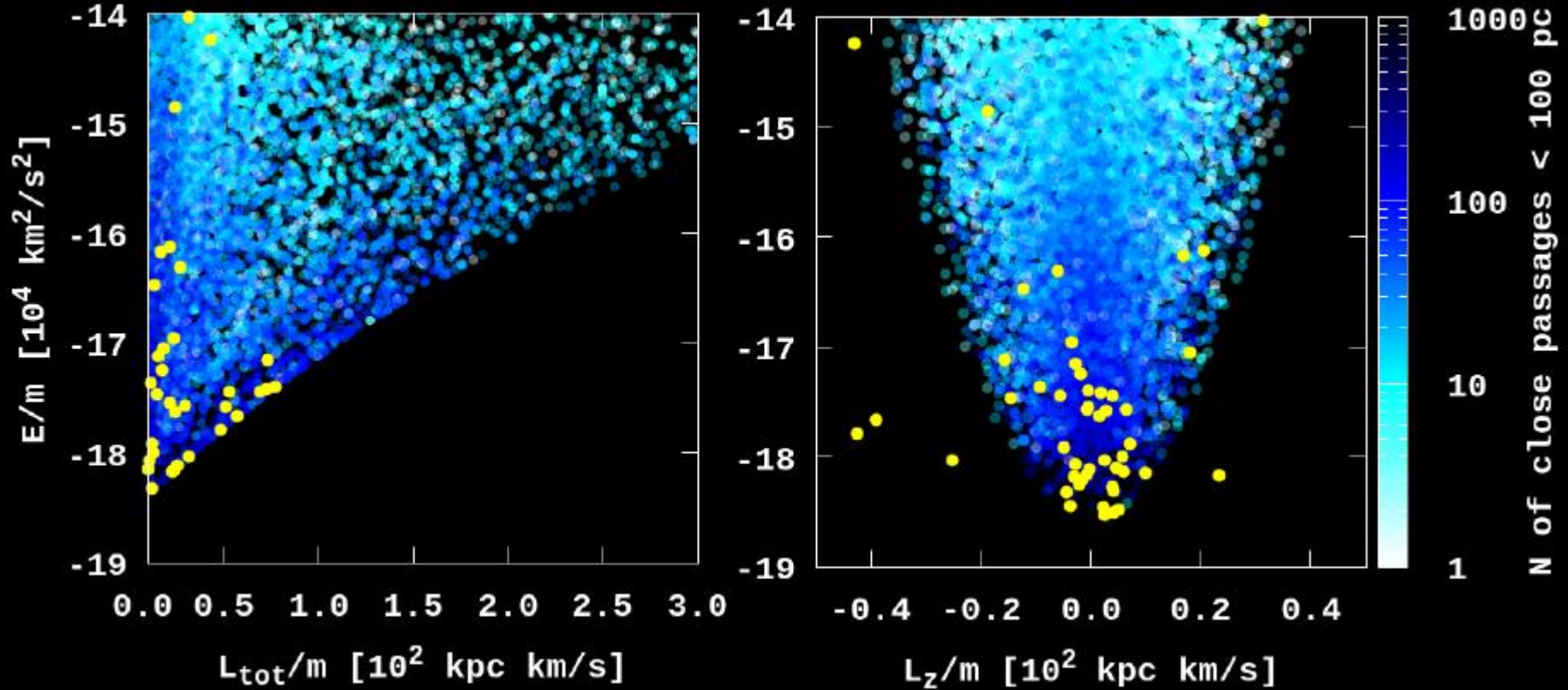


Distribution of the GCs in phase space: E vs. L_{tot} and E vs. L_z in 411321 external potential at -10 Gyr ago.

Colour-coding shows orbital mean ecc based on 5 Gyr of integration. More than 16k models.



Orbital evolution during 5 Gyr of integration, from -10 Gyr, represents orbits with different ecc, from 0.0 to 0.9.



Distribution of the GCs in phase space: E vs. L_{tot} , E vs. L_{perp} and E vs. L_z in 411321 external potential. Panels represent models, which have interaction (close passages) with the GalC, based on 5 Gyr of integration. Colour-coding represents the number of such events. Yellow dots represent selected GCs for future N-body simulations.

To carry out the N -body modelling together with the stellar evolution for early GCs, we assumed the initial conditions listed below:

- For the dynamical orbital integration of GCs, including the effects of stellar evolution, we employed the high-order parallel N -body code φ -GPU, which is based on the fourth-order Hermite integration scheme with hierarchical individual block time steps.
- For the individual mass of the stars, we used the Kroupa initial mass function (IMF; [Kroupa 2001](#)) with lower-upper mass limits equal to $0.08\text{--}100 M_{\odot}$.
- Each cluster was initially set in a state of dynamical equilibrium with King model distribution function ([King 1966](#)), the half-mass radius r_{hm} , and the dimensionless central potential W_0 .
- Initial coordinates and velocities at the -10 Gyr lookback time were taken from the orbital integration of the GC.

As an initial model for the Galactic NSC we include a special central proto-NSC particle with a mass of $4 \times 10^6 M_{\text{Sun}}$ and a radius of 10 pc in our simulations.

During the N-body simulation, we assume that a star from the GC has accreted to the NSC when the particular GC star is inside the 10 pc radius of the proto-NSC.

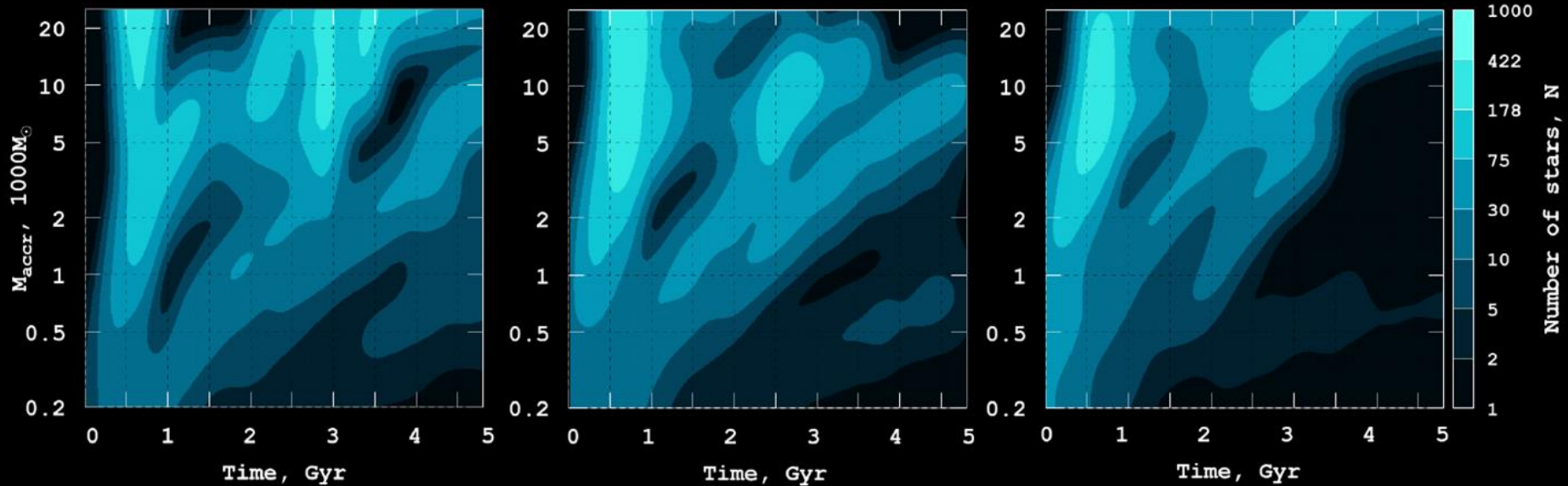
When such a star is detected, we add the current mass of the star at the time of the pass to the NSC and consider the star to be accreted. In such a case, we will always have a growing NSC mass.

Time integration is 5 Gyr, from -10 to -5 in a past.

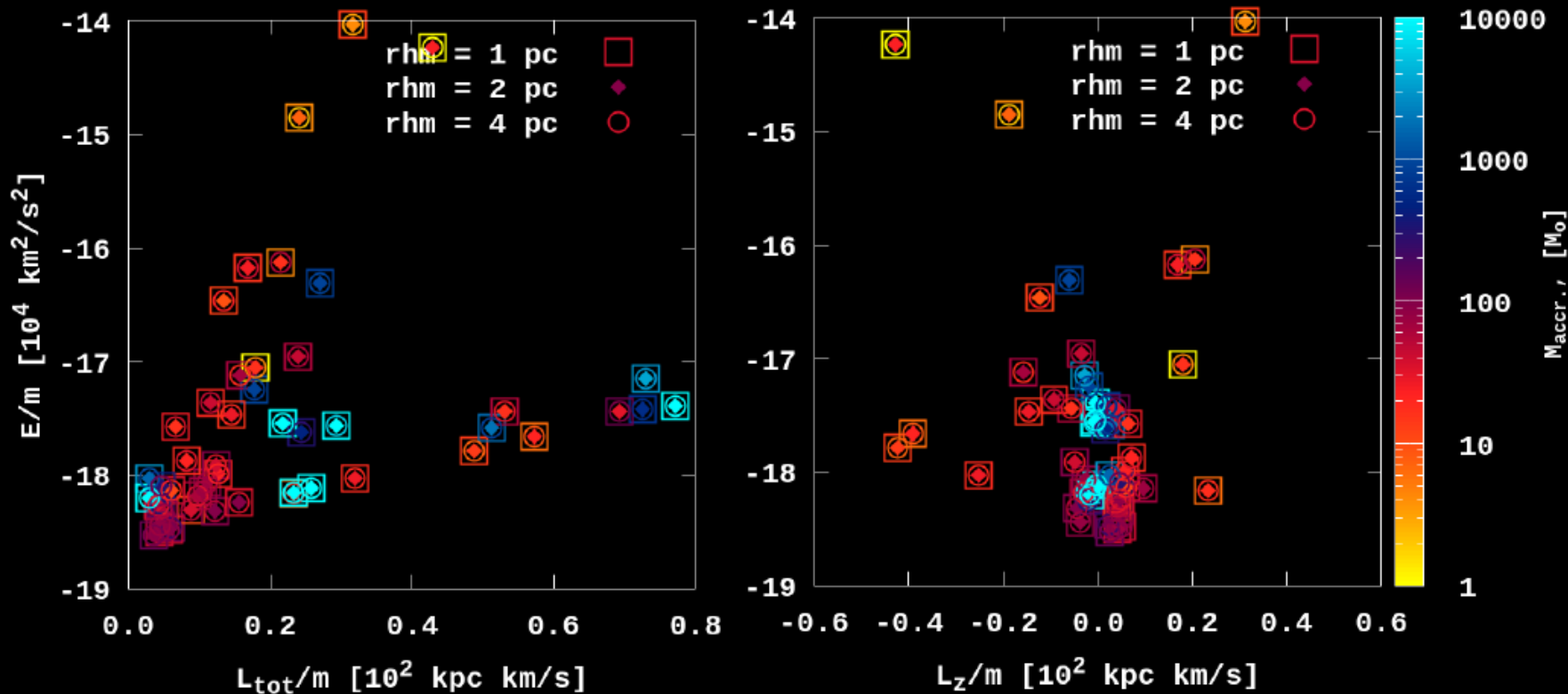
Initial physical parameters for GC's N-body modelling

No	M, M_{\odot}	N	r_{hm} , pc	W_0
50	60 000	104 554	1	8.0
50	60 000	104 554	2	8.0
50	60 000	104 554	4	8.0

Stellar accretion rates onto the NSC for 50 GCs models for three different values of $r_{\text{hm}} = 1, 2, \text{ and } 4 \text{ pc}$, respectively

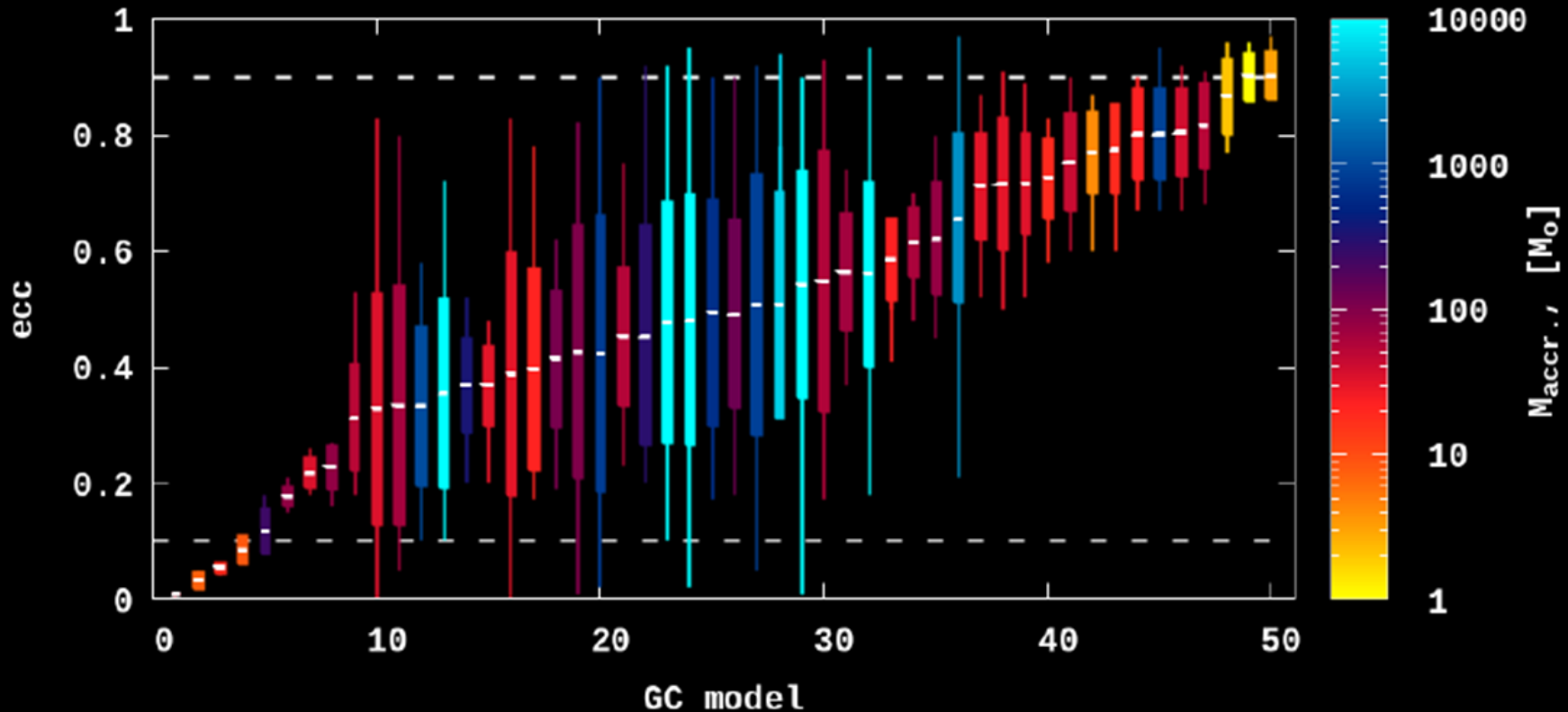


r_{hm}	N_{accr}	$M_{\text{accr}}, M_{\odot}$
1 pc	398 358	152 758
2 pc	309 987	117 981
4 pc	312 964	124 344



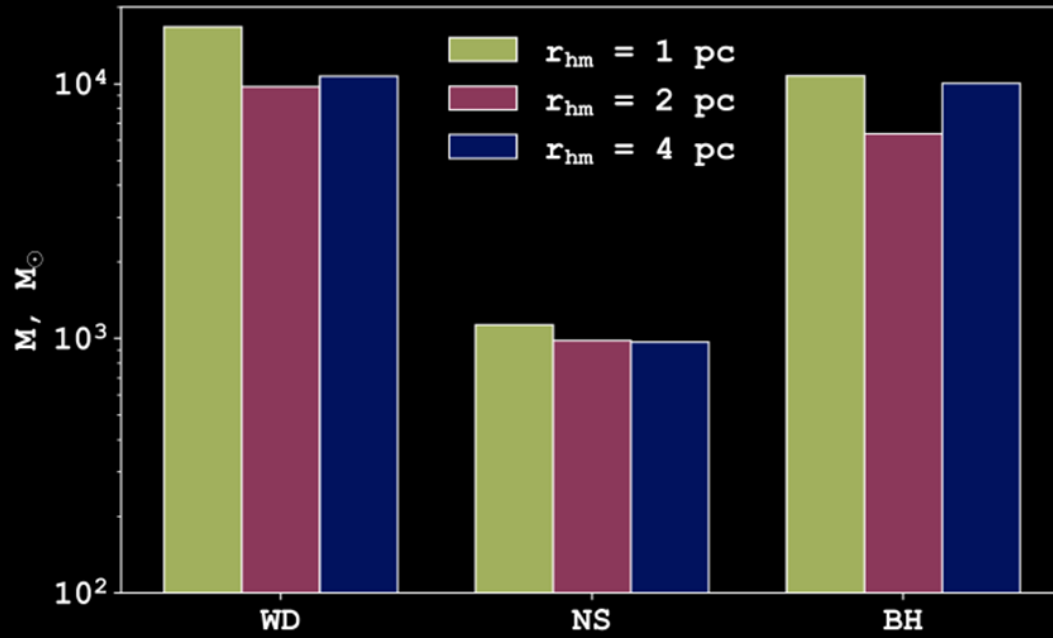
Initial distribution for 50 theoretical GCs in E – Ltot, and E – Lz at -10 lookback time. Different symbols show r_{hm}. Colour represent accreted mass from each GC to the NSC over 5 Gyr of integration time.

Evolution of the mass accretion to the NSC for models with r_{hm} depends on the ecc



Short black lines – mean values, colour box – $\pm 1\sigma$ for ecc, thin colour lines – minimum and maximum ecc values during 5 Gyr of integration. Colour – accreted mass to the NSC.

Accretion rate for the stellar remnants from GCs

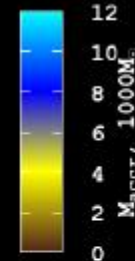
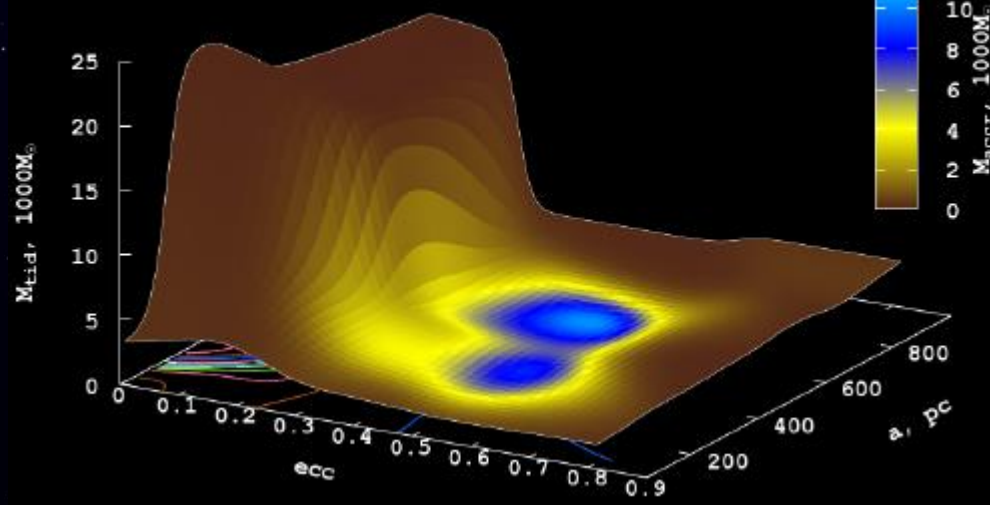
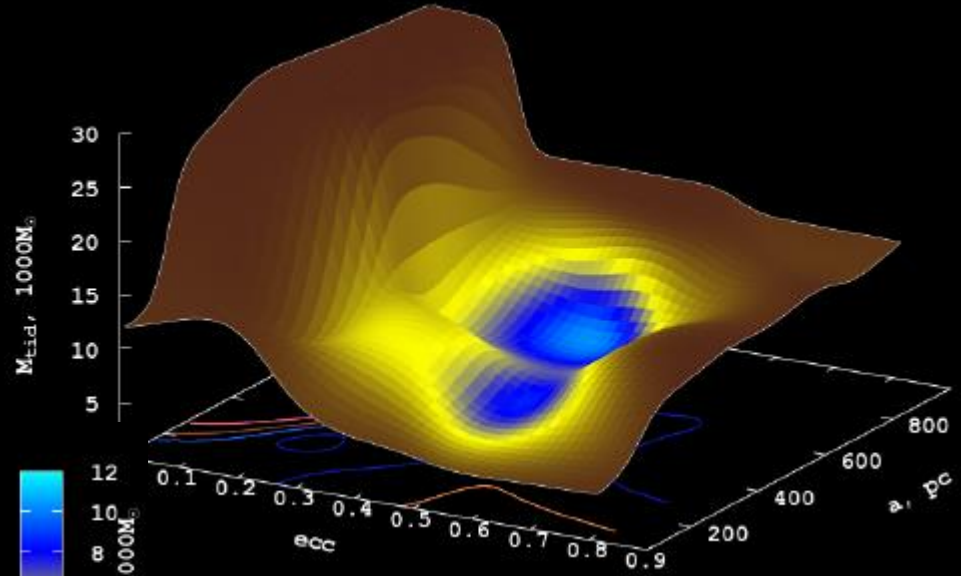
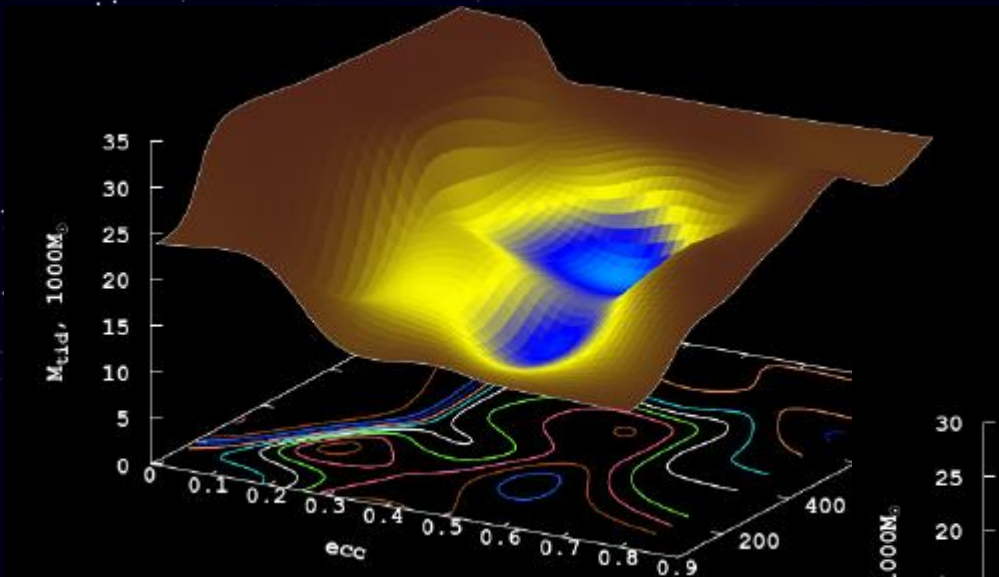


Total accretion of the mass of stellar remnants (WD, NS, and BH) from 50 GCs for all the three cases: $r_{hm} = 1, 2,$ and 4 pc. The mass in logarithmic scale.

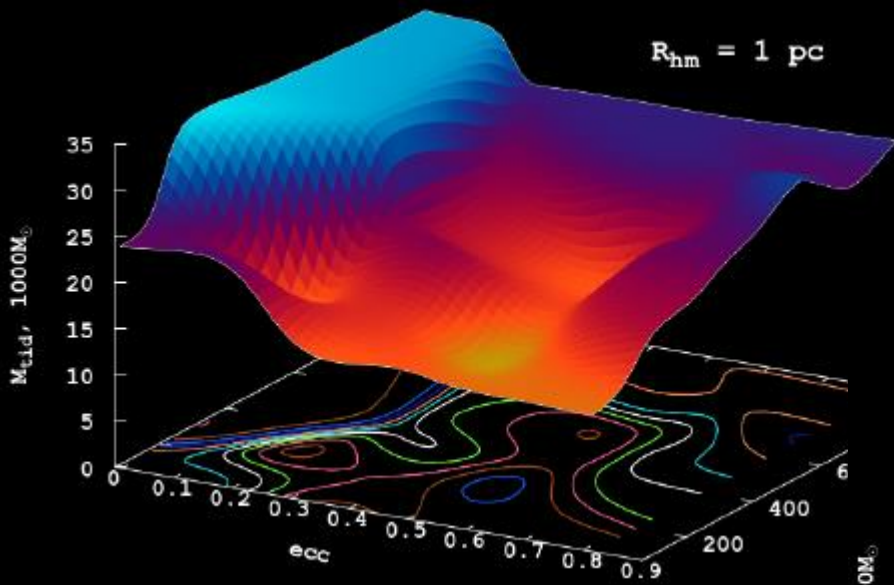
Accretion of the stellar remnants onto the NSC for sets of GCs with different initial r_{hm} , where mass accretion in M_{\odot}

r_{hm}	WD		NS		BH	
	N_{accr}	M_{accr}	N_{accr}	M_{accr}	N_{accr}	M_{accr}
1 pc	19 765	16 719	909	1 131	546	10 752
2 pc	10 957	9 732	785	979	336	6 359
4 pc	12 275	10 688	779	965	508	10 072

Accretion mass maps over all our theoretical GC models.

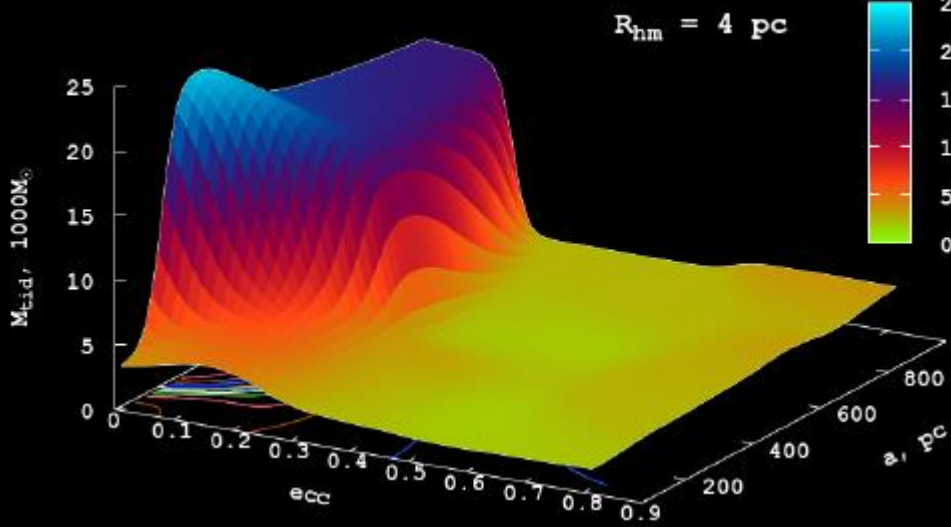
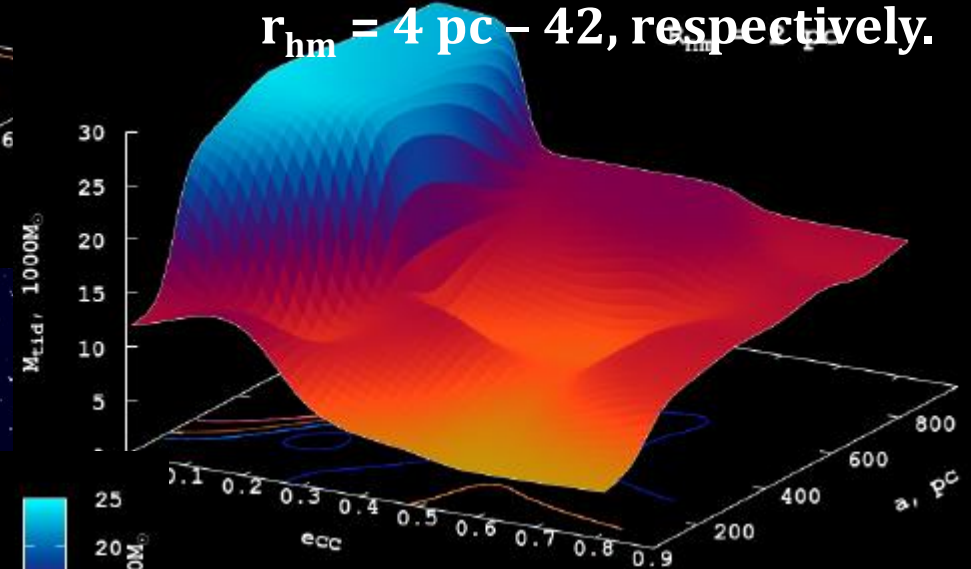


In most cases the dissolution of the GCs occurs in the models with the orbital ecc in a range of 0.4–0.5.



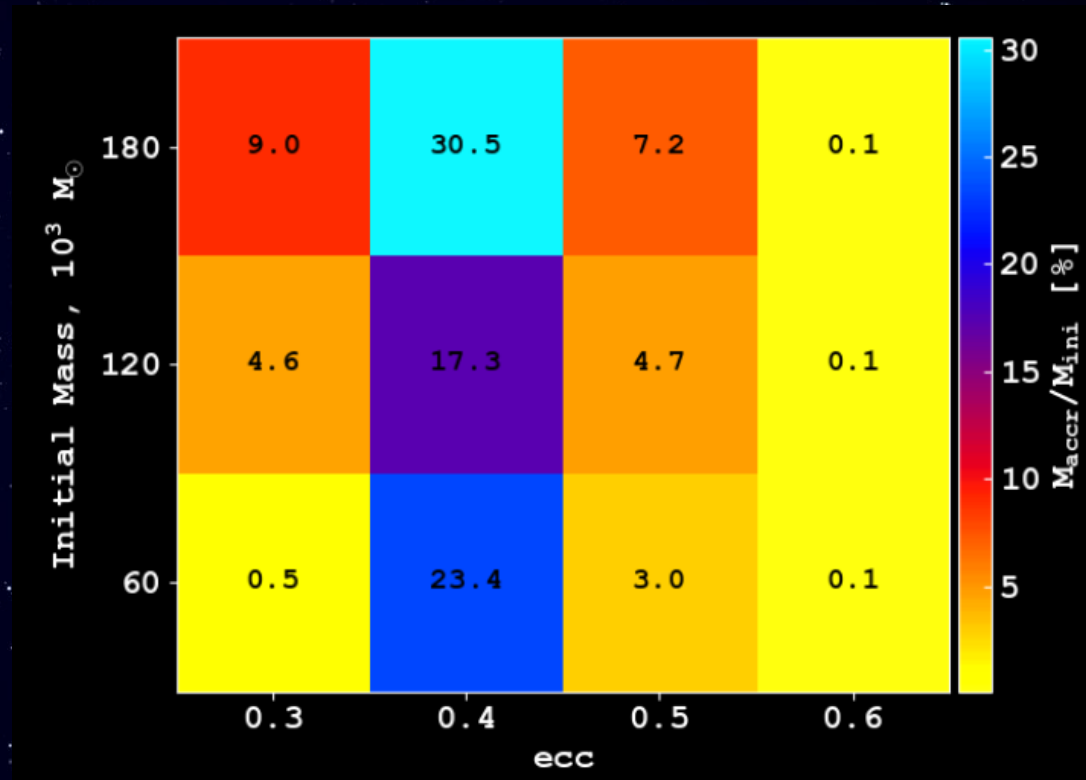
With initial $r_{hm} = 1 \text{ pc}$ we have 5 dissolved GCs during this 5 Gyr integration period. With initial $r_{hm} = 2 \text{ pc}$ we have 9 GCs, and with $r_{hm} = 4 \text{ pc} - 42$, respectively.

GCs mass loss



In most cases the dissolution of the GCs occurs in the models with the orbital ecc in a range of 0.3–0.6.

Role of the GC's mass loss and accretion rate for low and heavy cases




- The relative fractions of the accreted mass and the number of particles are given as percentages with respect to their initial values.
- As the initial mass of the GC models increases, their total mass contribution to the proto-NSC also grows.
- However, if we consider the ratio of initial masses to accreted masses for massive globular clusters, we can see that the increase is insignificant.

Conclusions:

- ✓ Based on the total accreted mass from all the three sets of our theoretical 150 GCs during the first 5 Gyr of Galactic evolution we accreted on the forming NSC $\sim 4 \times 10^5 M_{\odot}$. **This mass is roughly 2% of our current NSC mass $\sim 2 \times 10^7 M_{\odot}$**
- ✓ GC models with average orbital eccentricities of **0.4–0.5 and orbits oriented perpendicular to the galactic disk contribute most significantly to the mass of the proto-NSC formation.**
- ✓ Accretion is especially efficient during the first Gyr and in compact GC models with $r_{\text{hm}} = 1$ pc. In all sets, the dominant accreted stellar population consists of low-mass stars ($\approx 0.33 M_{\odot}$).
- ✓ Our accretion mass estimation is a lower limit, due to the absence of the dynamical friction prescription in our N-body modelling and the absence of the bulge model in the MW-like external potential.
- ✓ Based on our extended set of numerical simulations, we obtain the lower limit of mass contribution to the NSC from disrupted GCs. **We conclude that the GC stellar accretion channel alone may not be sufficient to ensure the present day MW galaxy NSC mass budget.**

How our proto Nuclear Star Cluster formed and grew due to early globular clusters disruption

D. Kuvatova^{1,2,3} , M. Ishchenko^{4,1,2} , P. Berczik^{1,2,6,4} , O. Veles^{4,1} , O. Sobodar^{4,1} , and T. Panamarev^{5,2} 

¹ Nicolaus Copernicus Astronomical Centre Polish Academy of Sciences, ul. Bartycka 18, 00-716 Warsaw, Poland

² Fesenkov Astrophysical Institute, Observatory 23, 050020 Almaty, Kazakhstan

³ Faculty of Physics and Technology, Al-Farabi Kazakh National University, al-Farabi ave. 71, 050040 Almaty, Kazakhstan

⁴ Main Astronomical Observatory, National Academy of Sciences of Ukraine, 27 Akademika Zabolotnoho St, 03143 Kyiv, Ukraine

⁵ Rudolf Peierls Centre for Theoretical Physics, Parks Road, OX1 3PU, Oxford, UK

⁶ Konkoly Observatory, Research Centre for Astronomy and Earth Sciences, HUN-REN CSFK, MTA Centre of Excellence, Konkoly Thege Miklós út 15-17, 1121 Budapest, Hungary

Thanks for your attention

